Modeling and Control of Magnetic Bearings with Nonlinear Magnetization

Ali Gerami, Paul Allaire, Roger Fittro

Ph.D. Candidate Dept. of Mechanical and Aerospace Eng., University of Virginia Charlottesville, VA 22903, ag4nt@virginia.edu
Chief Technical Officer, Rotor Bearing Solutions International, Charlottesville, VA 22903, paul.allaire41@gmail.com
Associate Director, Romac laboratory, Dept. of Mechanical and Aerospace Engineering University of Virginia, Charlottesville, VA 22903, rlf9w@virginia.edu,

***Abstract*- In this paper a nonlinear modeling approach is proposed to operate magnetic bearings above the linear range and near the material saturation point. The goal is to get higher load capacity from an existing AMB system by just changing the software. In order to do this, the system should be operated in the nonlinear region of the magnetization curve and therefore should be modeled nonlinearly. Simulation results show approximately twice the force capability. The controller designed using this approach has a much better transient response and domain of attraction.**

***Keywords*- Nonlinear Modeling; Magnetic Bearing; Generalized Lur'e Method; Linear Matrix Inequalities; Balance Beam**

I. INTRODUCTION

In this paper we introduce a new nonlinear modeling and control method to increase the load capacity of magnetic bearings. To increase the load, the electric current must be increased. This extra electric current and therefore extra flux density makes the system highly nonlinear. Therefore there is a need for a nonlinear model that can accurately model these higher operating conditions. Since it is a common industrial practice to include amplifiers with more capacity than needed for AMB systems as a safety factor, our proposed method can potentially increase the load capacity by just a change in the software. Therefore the proposed method can offer a low cost solution for occasional harsh situations with high transient loads that need to be handled by the AMB. In this study, a nonlinear model for magnetic journal bearings is developed considering the core material nonlinear behavior. This nonlinear behavior is shown in Fig. 1.

Extensive research has been reported to take into account AMB nonlinearities. The force created by an electromagnet is proportional to the square of the electric current and inversely proportional to the square of the air-gap between the rotor and the stator. The AMB force is thus nonlinear, and leads to some complexities in control synthesis. Much research has been devoted to the synthesis of such control laws. The majority of the research in nonlinear AMB's has considered current and airgap nonlinearity. The research done by Yin [1], Inoue [2], Abdelfatah [3], Hong [4], Smith [5] are just a few examples. The force, displacement, and current relationship have usually been studied in single-DOF systems. Walsh [6] considered the geometric coupling of a 2-DOF AMB and studied the changes in stiffness and the resulting bifurcation. Abdelfatah [3] studied the nonlinear oscillations caused by the gyroscopic effect. He [7] and Huang [8] modeled and controlled 5 and 6-DOF systems. Other researches have considered geometric nonlinearities by Hu [9], amplifier nonlinearities by Inoue [2], hysteresis by Wang [10] and control system delays by Tsuyoshi [2,11] and Zheng [12,13]. More recently, self-sensing magnetic bearings by Noh [14] and contact between rotor and the auxiliary bearing by Foiles [15] have been studied. Steinschaden [16] and some others considered the magnetic flux saturation by using a simple bilinear model. Widger [17] and Rivas [18] incorporated the material saturation by curve fitting. Even though magnetization nonlinearity is modeled in some of the previous work, these models are not used for controller development. In this paper, the magnetization nonlinearity is modeled precisely, using the Lur'e method. This method makes the model more suitable for control design, which in turn enables the design of controllers that significantly improve the load capacity of the system.

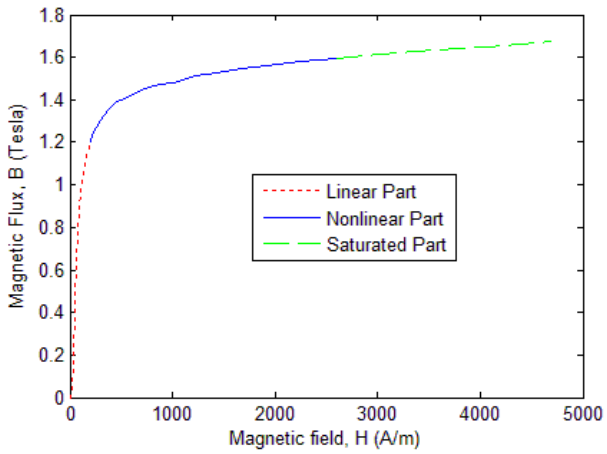

Fig. 1 Silicon iron magnetization curve

II. Dynamic Model and Constraints

A. Introduction

In this paper a balance beam is used for dynamic modeling and simulation. The mechanical part is basically a beam free to rotate on a pivot. The angle of the beam with the horizon is controlled by the two electromagnets on both ends of the beam. This system emulates the dynamics of a single DOF thrust magnetic bearing. The equation of motion can be written as follows:

$$J\ddot{\theta} = -D\dot{\theta} + L_a\left(F_2 - F_1\right) \tag{1}$$

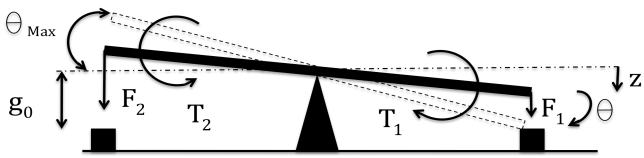

Fig. 2 The balance beam

Here J is the mass moment of inertia of the beam, θ is the angle between the beam and the horizontal direction. D is the system damping due to the pivot and air friction. F_1 and F_2 are the left and right electromagnetic forces and L_a is the distance between electromagnets and pivot (see Fig. 2).

B. Nonlinear Force Model

Since the proposed model works in the nonlinear B-H region, the flux density is very high and the magnetic reluctance of the core material cannot be neglected. Therefore the flux density in the electromagnets can be calculated as follows:

$$B_{1,2} = \frac{NI_{1,2}}{\frac{2(g_0 \pm z)}{\mu_0} + \frac{L_s}{\mu_r}} \tag{2}$$

Here B_1 and B_2 are the flux density of the electro magnets, L_s is the length of silicon iron in the magnetic circuit, N is the number of turns in each coil, μ_0 is the permeability of free space, μ_r is the relative permeability of silicon iron, g_0 is the airgap, $I_1 = I_b + I_c$ and $I_2 = I_b - I_c$ are the electric currents, I_c is the control current, I_b is the bias current, L_s/μ_r is the magnetic reluctance of the silicon iron, and $2g_0/\mu_0$ is the magnetic reluctance of the airgap.

In the nonlinear region of the B-H curve the relative permeability of the silicon iron can be modeled as follows:

$$\mu_r = aB + b \tag{3}$$

Here a and b are two constants that were found by curve fitting on the nonlinear region of the B-H curve. The actuator force is related to the flux density by the following equation:

$$F = \frac{A}{\mu_0}B^2 \tag{4}$$

By using a combination of Eqs. 2,3, and 4, the force of each electromagnet can be calculated using the following equations:

$$F_1 = \frac{1}{g_0^2\left(1 - \frac{2z}{g_0}\right)}\left[\begin{matrix} c_1 I_1^2 - c_2 z + c_3 \\ +\left(c_4 I_1 - c_5 z + c_6\right)\sqrt{c_7 I_1^2 + c_8 I_1 z - c_{10} z + c_{11}} \end{matrix}\right] \tag{5}$$

$$F_2 = \frac{1}{g_0^2\left(1 + \frac{2z}{g_0}\right)}\left[\begin{matrix} c_1 I_2^2 + c_2 z + c_3 \\ +\left(c_4 I_2 + c_5 z + c_6\right)\sqrt{c_7 I_2^2 + c_8 I_1 z + c_{10} z + c_{11}} \end{matrix}\right] \tag{6}$$

Here $c_1, c_2, \ldots, c_{11}$ are constants based on system parameters and they can be found in the appendix. z is the displacement of the end of the beam. These force equations are valid for the nonlinear part of the B-H curve. For the linear part of the B-H curve, the conventional equations are used. Figure 3 shows that the proposed nonlinear model closely matched the manufacturer material data. The balance beam dimensions and other physical parameters are listed in Table 1.

Table 1-Balance beam parameters

	Parameter	Value
L_a	Electromagnet distance from the pivot	0.1667 m
D	Pivot friction coefficient	0 Ns/m
J	Moment of inertia	16.32 gm^2
N	Number of turns per coil	110 Turns
g_0	Airgap	0.397 mm
L_s	Distance the flux travels inside the core	0.178 m
I_b	Bias current	1.55 A
K_s	Stiffness	1236540 N/m
I_{max}	The maximum electric current	9.61 A
θ_{max}	The maximum angle of rotation	0.0024 Rad

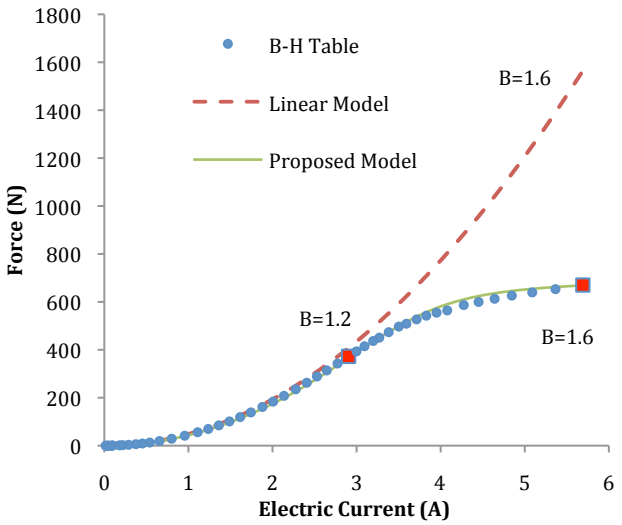

Fig. 3 Each electromagnet's force vs., coil current

III CONTROL

The Lur'e method was used for nonlinear modeling. The control problems described by the Lur'e method have a forward path that is linear and time-invariant, and a feedback path that contains a memoryless, possibly time-varying, nonlinearity (see Fig. 4). In the figure, A is the state matrix, B_u is the input matrix, B_w is the disturbance input matrix, and C_y is the output matrix. This method breaks the nonlinear model into linear and nonlinear parts, which simplifies the control synthesis process.

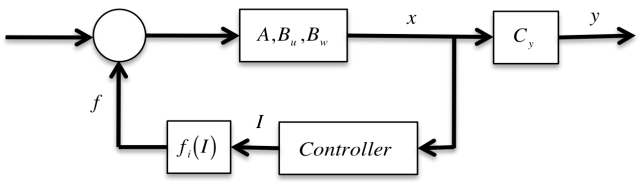

Fig. 4 Balance beam in terms of Lur'e problem

The total balance beam force can be calculated as follows:

$$F = K_s z + f_i(I_c) \tag{7}$$

$$z = L_a \theta \tag{8}$$

Here, F is the net actuator force ($F = F_1 - F_2$). K_s can be obtained by linearizing the force around its equilibrium point, and $f_i(I_c)$ is the nonlinear force due to the electric current assuming no displacement. The balance beam can be modeled into the Lur'e system formulation as follow,

$$\begin{bmatrix} \dot{\theta} \\ \ddot{\theta} \end{bmatrix} = \begin{bmatrix} 0 & 1 \\ \frac{L_a^2 K_s}{J} & -\frac{D}{J} \end{bmatrix} \begin{bmatrix} \theta \\ \dot{\theta} \end{bmatrix} + \begin{bmatrix} 0 \\ \frac{L_a}{J} \end{bmatrix} f_i \tag{9}$$

In terms of the Lur'e problem, $f_i(I_c)$ is the nonlinear input and should therefore satisfy the sector condition. The sector condition constraints the system within two sector bounds which normally are two straight lines. In addition to the regular sector condition, the generalized sector condition that is developed by Lin et al. [19] is used in this work (see Fig. 5). The generalized condition includes using two segmented lines instead of two straight lines, which enables the resulting control design to be less conservative.

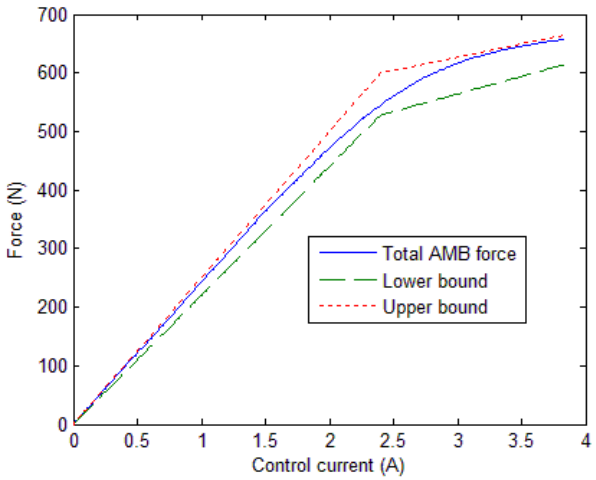

Fig. 5 Generalized sector condition

In addition to the sector condition, there are other physical constraints that need to be satisfied to make sure 1) the beam will not contact the electromagnets, 2) the coils will not overheat, 3) and the total current in each electromagnet is positive. These conditions are expressed mathematically as follows:

$$|I_c| \le I_{\max} \tag{10}$$

$$I_1, I_2 > 0 \tag{11}$$

$$|\theta| \le \theta_{\max} \tag{12}$$

Here $I_{\max}$ is the maximum tolerable current without overheating the coil and $\theta_{\max}$ is the beam's maximum allowable rotation angle.

IV RESULTS

By using linear matrix inequalities and linear programming, an optimized control for the system of Equations (9) is designed that satisfies the physical constraints. The conventional linear model is compared to the nonlinear model with both normal and general sector conditions. The first objective was to obtain the largest possible domain of attraction (invariant ellipsoid). In other words, a controller is designed that can provide the largest initial angular displacement which also ensures system stability. The following optimization problem is solved to achieve this objective:

$$\begin{aligned}
&\sup_{P>0,F} \alpha \\
&(a)\ \ \alpha x_i \in \varepsilon(P), i = 1,2,\cdots,l \ \ and \ \ x_i \in X_0 \\
&(b)\ \ (A + k_1 BF)^T P + P(A + k_1 BF) \le 0 \\
&\qquad (A + k_2 BF)^T P + P(A + k_2 BF) \le 0 \\
&(c)\ \ \varepsilon(P) \subset L(F) \\
&(d)\ \ \varepsilon(P) \subset L(G)
\end{aligned} \tag{13}$$

Here, P is a positive definite variable, $\varepsilon(P)$ is the invariant ellipsoid, and G is the state constraint matrix which in here can be defined as $G = [1/\theta_{\max} \ \ 0]$. In Part (a) of the optimization problem of Equation (12), the x_i's are chosen points that determine the shape of the domain of attraction (the ratio of the major and minor axis of the invariant ellipsoid). The optimization problem maximizes α which corresponds to the size of the invariant ellipsoid. Part (b) guarantees the stability of the system on the normal sector bounds. k_1 and k_2 are the slopes of the two sector bounds. For generalized sector bounds the following constraint should be used instead of constraint (b):

$$\begin{aligned}
&b1)\ \ (A + k_{0m} BF)^T P + P(A + k_{0m} BF) < 0 \\
&b2)\ \ (A + BH_{im})^T P + P(A + BH_{im}) < 0, \ i \in I[1,N] \\
&b3)\ \ \varepsilon(P) \subset \bigcap_{i=1}^{N} L\left(\frac{H_{im} - k_{im} F}{c_{im}}\right)
\end{aligned} \tag{14}$$

Here, H_{im} is a new variable in the optimization problem, k_{im} is the slope of different segments of the sector bound and c_{im} is the y-intercept of these segments. For example k_{31} is the slope of the fourth segment of the first sector bound and c_{12} is the y-intercept of second segment of the second sector bound. For the first segment $i = 0$ and since it passes through the origin, the y-intercept is zero.

Part (c) and part (d) define the amplifier and state constraints respectively. The domain of attraction and the constraints are depicted in Fig. 6. Three different control designs are compared. "Nonlinear Regular" is the domain of attraction of the system under a feedback control that is designed using the nonlinear model with regular sector conditions; "Nonlinear Generalized" is the domain of attraction of the system under the controller designed using the nonlinear model with generalized sector conditions, and "Jacobean" marks the domain of attraction obtained by a controller designed based on the linear Jacobean model.

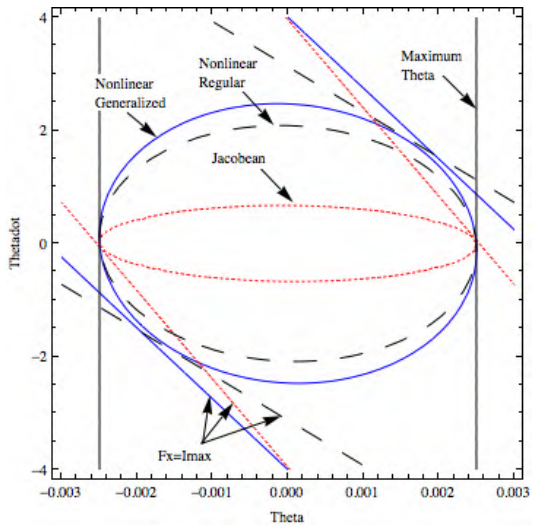

Fig. 6 Domain of attraction for linear and nonlinear models

The sloped lines represent the constraint imposed by the maximum possible electric current. By using the nonlinear model, these constraints are less restrictive and allow larger initial velocities.

The second objective was to obtain the fastest transient response. To achieve this objective the following optimization problem is solved:

$$\sup_{P>0,F} \beta$$

$$(a)\ \ x_i \in \varepsilon(P), i = 1,2,\cdots,l \ \ and \ \ x_i \in X_0$$

$$(b)\ \ (A + k_1 BF)^T P + P(A + k_1 BF) \le -\beta P$$

$$(A + k_2 BF)^T P + P(A + k_2 BF) \le -\beta P \qquad (15)$$

$$(c)\ \ \varepsilon(P) \subset L(F)$$

$$(d)\ \ \varepsilon(P) \subset L(G)$$

The various parts of this optimization problem represent the same constraints as the previous optimization problem, but here a larger β represents a better transient response. Therefore β is optimized. As for the previous optimization problem, to use the generalized sector condition, Equation (14) should replace condition (b) in Equation (15). The results show that using the nonlinear model can significantly improve the transient response of the system (see Fig. 7). Systems responses to a step input and zero initial conditions are shown in Figure 7. As can be seen, the two controllers that are designed using the nonlinear model have significantly better transient responses. These control designs result in approximately half of the settling time compared to the linear model, which is a significant improvement.

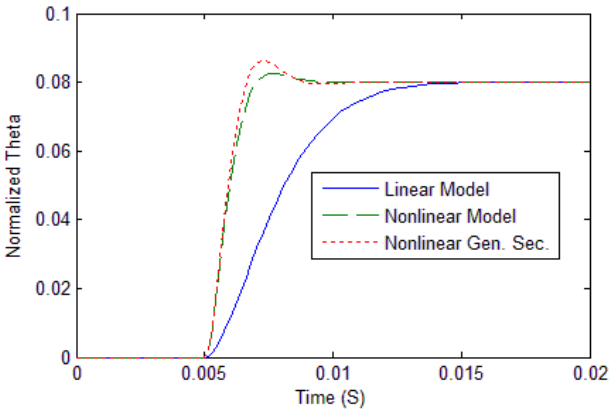

Fig. 7 Transient response of linear and nonlinear models

V CONCLUSIONS

In this paper a new nonlinear model using modeling material magnetization in AMBs was proposed for the first time. State and input constraints were also considered in modeling. LMI optimization and the Lur'e method were utilized for control synthesis. Simulation results illustrate a larger domain of attraction. Also the proposed model enabled controllers to be designed with significantly better transient response. In general, the proposed model provides the system with extra force when it is needed. More importantly, these improvements can be achieved by only changing the control algorithm and no change in the hardware is necessary. This extra capability can potentially be used to design smaller, lighter, and more reliable magnetic bearings.

APPENDIX

Force constants:

$$c_1 = \frac{A\mu_0}{8N^2}, \qquad c_2 = \frac{a(L_1 + L_2)A + 2a^2 A g_0}{2\mu_0 b^2}$$

$$c_3 = \frac{A(L_1 + L_2)^2 + 4a(L_1 + L_2)Ag_0 + 4a^2 Ag_0}{8\mu_0 b^2}$$

$$c_4 = \frac{AN}{2}, c_5 = \frac{aA}{b\mu_0}, c_6 = \frac{A(L_1 + L_2) + 4Aag_0}{4b\mu_0}$$

$$c_7 = \frac{\mu_0^2}{16N^2}, \qquad c_8 = \frac{\mu_0 N(2ag_0 - L_1 - L_2)}{8b}$$

$$c_9 = \frac{\mu_0 Na}{4b}, \qquad c_{10} = \frac{a(L_1 + L_2) + 2a^2 g_0}{4b^2}$$

$$c_{11} = \frac{(L_1 + L_2)^2 + 4a(L_1 + L_2)g_0 + 4a^2 g_0^2}{16b^2}$$

REFERENCES

[1] Yin, Lingbing, and Lei Zhao. "Nonlinear Control for a Large Air-gap Magnetic Bearing System." Proc. of SMiRT 19, Toronto. N.p.: n.p., n.d. N. pag. Web. Aug. 2007.

[2] Inoue, Tsuyoshi, Yukio Ishida, and Shin Murakami. "Theoretical Analysis and Experiments of the Nonlinear Vibration in a Vertical Rigid Rotor Supported by the Magnetic Bearing System." *Ournal of System Design and Dynamics* 1.2 (n.d.): 295-306. Web. 2007.

[3] Abdelfatah, Mohamed M., and Emad P. Fawzi. "Nonlinear Oscillations in Magnetic Bearing Systems." *Ieee* 8th ser. 38 (1993): 1242-245. Print.

[4] Hong, Sung K., and Reza Langari. "Fuzzy Modeling and Control of a Nonlinear Magnetic Bearing System." *Journal of Intelligent & Fuzzy Systems* 7.4 (1999): 335-46. Print.

[5] Smith, R. D., and W. F. Weldon. "Nonlinear Control of a Rigid Rotor Magnetic Bearing System: Modeling and Simulation with Full State Feedback." *Ieee* 31.2 (1995): 973-80. Print.

[6] Walsh, Thomas F. *Nonlinear Dynamic Analysis of a Magnetic Bearing System with Flux Control: The Effects of Coordinate Coupling*. N.p.: DukeUniversity, 1993. Print.

[7] He, Rong, Kang Z. Liu, and Osami Saito. "Nonlinear Output Feedback Control of a 5DOF AMB System." Proc. of 16th IFAC World Congress, Czech Republic. Vol. 16. N.p.: n.p., 2005. N. pag. Print. Ser. 1.

[8] Huang, Shi J., and Lih C. Lin. "Stable Fuzzy Control with Adaptive Rotor Imbalance Compensation For nonlinear Magnetic Bearingsystems." *Journal of the Chinese Institute of Engineers* 4th ser. 28 (2005): 589-603. Print.

[9] Hu, Tingshu, and Zongli Lin. *Control Systems with Actuator Saturation: Analysis and Design*. Boston: Birkhäuser, 2001. Print.

[10] Wang, Yong, James D. Paduano, and Richard M. Murray. "BIFURCATION CONTROL: THEORIES, METHODS, AND APPLICATIONS." *IEEE* (1999): 730-36. Print.

[11] Inoue, Tsuyoshi, Motoki Sugiyama, Yasuhiko Sugawara, and Yukio Ishida. "Nonlinear Vibration in a Vertical Rigid Rotor Supported by the Magnetic Bearing: Case Considering the Delays of Both Electric Current and Magnetic Flux." *21st Biennial Conference on Mechanical Vibration and Noise / Modeling, Vibration and Control of Rotor*

Systems. Proc. of ASME, Nevada, USA, Las Vegas. Vol. 1. N.p.: n.p., 2007. 1195-203. Print.

[12] Zheng, Kai, Heng Liu, and Lie Yu. "Robust Fuzzy Control of A nonlinear Magnetic Bearing system with Computing Time Delay." *IEEE/ASME* (2008): 839-43. Print.

[13] Zheng, Kai, and Lie Yu. "Effects of Time Delay on Resonance of a Nonlinear Magnetic Bearing System with Delayed Feedback." *International Journal of Applied Electromagnetics and Mechanics* 3-4 33 (2010): 1547-554. Print.

[14] Noh, Myounggyu D., and Eric H. Maslen. "Self-Sensing Magnetic Bearings Using Parameter Estimation." *IEEE TRANSACTIONS ON INSTRUMENTATION AND MEASUREMENT* 46.1 (1997): 45-50. Print.

[15] Foiles, W. C., and P. E. Allaire. "Nonlinear Transient Modeling of Active Magnetic Bearing Rotors during Rotor Drop on Auxiliary Bearing." *Industrial Conference and Exhibition on Magnetic Bearings*. Proc. of MAG '97, Radisson Plaza Hotel at Mark Center, Alexandria, Virginia. N.p.: n.p., 1997. 154-63. Print.

[16] N. Steinschaden "Nonlinear Stability Analysis of Active Magnetic Bearings" *in fifth Int. Symp. Magnetic Suspension technology*, 1999, pp. 411-427.

[17] J. Rivas, J. M. Zamarro, E. Martin, and C. Pereira, "Simple approximation for magnetization curves and hysteresis loops," *IEEE Trans. Magn.,* vol. MAG-17, no. 4, pp. 1498–1502, Jul. 1981.

[18] G. F. T. Widger, "Representation of magnetisation curves over extensive range by rational-fraction approximations," *Proc. Inst. Elect. Eng.,* vol. 116, pp. 156–160, 1969.

[19] Huang, Bin, and Zongli Lin. "Absolute Stability With a Generalized Sector Condition." Automatic Control, IEEE 49.4 (2004): 535-48. Print.